Proceedings of the
5th ASME/JSME Joint Thermal Engineering Conference
March 15-19, 1999, San Diego, California

AJTE99-6513

FT-ICR STUDIES OF LASER DESORBED CARBON CLUSTERS

Shigeo MARUYAMA, Tetsuya YOSHIDA, Masamichi KOHNO and Mitsuru INOUE
Department of Mechanical Engineering
The University of Tokyo
7-3-1 Hongo, Bunkyo-ku, Tokyo 113-8656, Japan
maruyama@photon.t.u-tokyo.ac.jp

Keywords : Microscale Heat Transfer, Cluster, Laser, Mass Spectroscopy

ABSTRACT

Atomic and molecular clusters are being recognized as playing an important role in the thin-film deposition process and phase-change phenomena. Furthermore, small clusters are the most adequate system for the verification of quantum molecular dynamics calculations such as the interference of light and matter. Hence, experimental treatments of such atomic and molecular clusters are now desired. In order to examine such clusters, we have implemented a Fourier transform ion cyclotron resonance (FT-ICR) spectrometer directly connected to a laser-vaporization supersonic-expansion cluster beam source.

The heart of the FT-ICR spectrometer was made of ICR cell cylinder centered in a strong homogeneous magnetic field of a 6 Tesla superconducting magnet. The atomic cluster beam was generated outside of magnetic field by the laser vaporization of a solid sample disk, followed by cooling with supersonic expansion of pulsed helium gas. The ionized cluster was carried by helium gas and directly injected to the magnetic field. By measuring the ion-cyclotron frequency, which was inversely proportional to the ion mass, a very high-resolution mass spectrum can be obtained.

The high mass-resolution was demonstrated for positive mass spectra of silicon, carbon, and metal-carbon binary clusters and negative mass spectra of metal-carbon binary clusters. For bare carbon positive clusters, we found the special condition where the odd-numbered clusters were observed in the range of C_{30} to C_{50} and the continuous change to C_{60}-dominant condition and 'normal' even-numbered distribution.

An example of mass spectrum measured by the direct-injection FT-ICR apparatus is shown in Figure A-1. Here, a graphite sample with about 1 % of Sc, which is the typical composition used for macroscopic metal-containing fullerene, was vaporized by the 2nd harmonics of Nd: YAG laser and the positive clusters were trapped and analyzed by the FT-ICR spectrometer. If we ignore the metal-composite clusters, the distribution of bare carbon clusters was almost the same as typical pure carbon clusters. One the other hand, almost all of Sc-carbon composite clusters had only one Sc atom and even number of carbon atoms: ScC_{2n} in the range of $36 \le 2n \le 76$, with special magic numbers of ScC_{44}, ScC_{50}, ScC_{60}. These magic numbers were reproduced for La-C and Y-C binary clusters, even though the relative amount of bare carbon clusters were much less for La and Y.

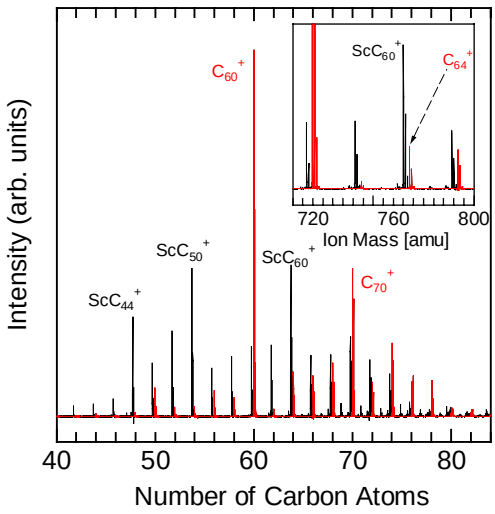

Figure A-1 A FT-ICR mass spectrum of Sc carbon binary clusters generated by the cluster source.

NOMENCLEATURE

B :	Magnetic field
f :	Ion cyclotron resonance frequency
m :	Mass of cluster ion
q :	Charge of cluster ion
r :	Radius of cyclotron motion
v :	Velocity

INTRODUCTION

Atomic and molecular clusters are being recognized as playing an important role in the thin-film deposition process and phase-change phenomena. Furthermore, small clusters are the most adequate system for the verification of quantum molecular dynamics calculations such as the interference of light and matter, since a cluster is the unique small atomic system with a physically clear boundary condition. Hence, experimental treatments of such atomic and molecular clusters are now desired.

Studies of clusters have another possibility leading to the discovery of new materials such as fullerene. Fullerene was first discovered in the mass-spectroscopic study by Kroto et al. (1985). Then, in 1990 the macroscopic generation by arc-discharge technique [Krätschmer et al. (1990), Haufler et al. (1991)] was introduced. Furthermore, higher fullerene [Kikuchi et al. (1992)], metal-containing fullerene [Chai et al. (1991), Kikuchi et al. (1993), Takata et al. (1995)] and nanotube [Iijima (1991), Thess et al. (1996)] were also generated by the similar technique. Even though the generation of fullerene is now possible by the arc-discharge technique or laser-oven technique [Haufler et al. (1991), Wakabayashi et al. (1997)], the formation mechanism of such spherical molecules is not clarified yet. In addition to our molecular dynamics studies [Yamaguchi & Maruyama (1998), Maruyama & Yamaguchi (1998), Yamaguchi et al. (1999)] for the generation mechanism, we come back to the mass-spectroscopic studies in this paper. Mass spectra of metal-carbon binary clusters are very complicated and we needed to implement a new FT-ICR (Fourier transform ion cyclotron resonance) spectrometer with extremely high mass-resolution. As our previous version at Rice University [Maruyama et al. (1990A), Maruyama et al. (1990B), Maruyama et al. (1991)], a laser-vaporization supersonic-expansion cluster beam source (Maruyama et al., 1997) was directly connected to the FT-ICR spectrometer. In this paper, the implementation of this new spectrometer with the cluster source is discussed together with the preliminary studies of pure-carbon and metal-carbon binary clusters.

FT-ICR MASS SPECTROSCOPY

The FT-ICR is the unique mass spectroscopy based on the ion-cyclotron motion of clusters in a strong magnetic field. In principle, extremely high mass-resolution at high mass-range such as resolution of 1 amu at 10,000 amu range should be possible. The heart of the FT-ICR spectrometer was made of ICR cell cylinder shown in Figure 1 centered in a strong homogeneous magnetic field of a 6 Tesla superconducting magnet. The design concept was the same as our previous version at Rice University (Maruyama et al., 1990A). The side plates of the ICR cell were composed of four sectors of a 42 mm i.d. cylinder, 150 mm in length. Two opposing 120° sectors were used for excitation of the trapped cluster ions, while the other two 60° sectors were used for detection of the image current induced by the cyclotron motion. There were conical-shaped 'front' and 'back' doors (with open inner diameter of 22 mm) in two longitudinal ends of the cell. When a cluster ion with mass m and charge q is placed in the homogeneous magnetic field of B, the Lorenz force induces

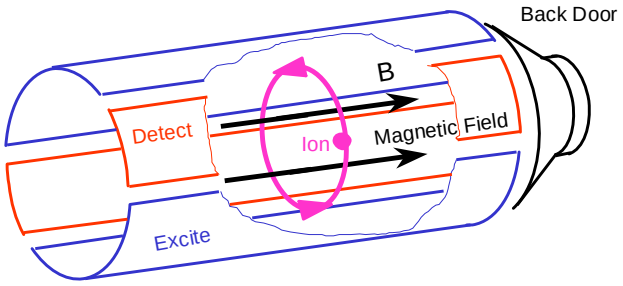

Figure 1 Schematics of ICR cell.

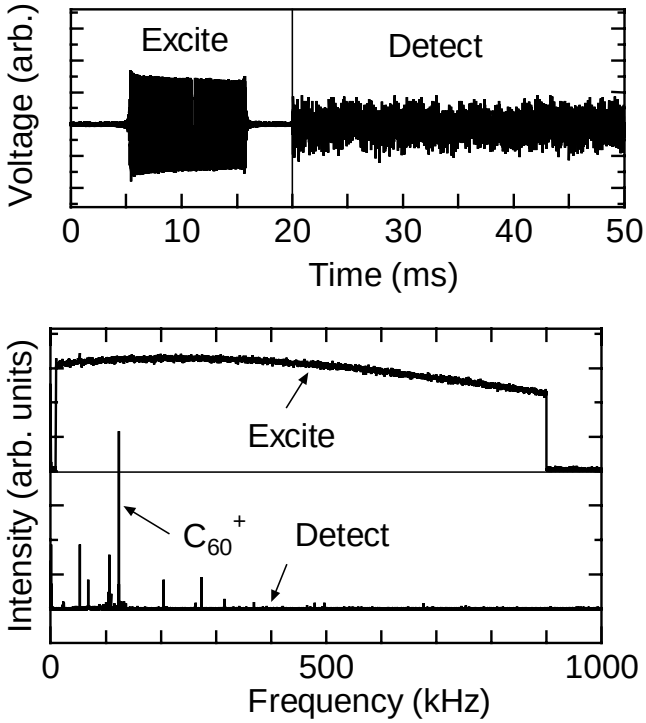

Figure 2 Example of excite and detect waveforms.

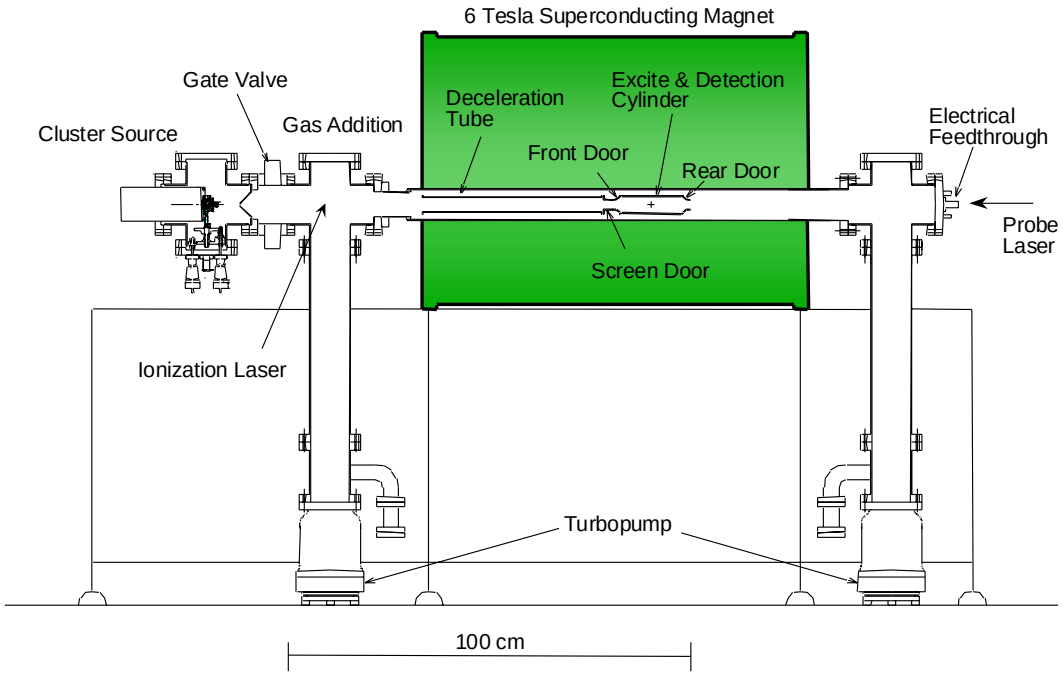

Figure 3 FT-ICR apparatus with direct injection cluster beam source

the ion cyclotron motion. The centrifugal force is $mv^2/r = qvB$, where v is velocity and r is the radius of the cyclotron motion. The frequency $f = qB/2\pi m$ is determined by the ratio of charge and mass q/m.

In order to measure the mass spectrum, the ion cyclotron motion of a packet of cluster ions was excited by the oscillating electrical field. When the radius of the cyclotron motion became as large as the detection cylinder, the induced current due to the motion of the ion packet on detection plates were measured through a differential amplifier. As an example, Figure 2 shows the excitation and detected waveforms both in time and frequency domains. The excitation waveform was generated by the inverse Fourier transform of arbitrary shape in the frequency domain: called SWIFT (stored waveform inverse Fourier transform) technique [Marshall et al. (1985), Marshall & Verdun (1990)]. In Figure 2, the frequency range of 10 kHz - 900 kHz were uniformly excited. 'Excite' signal in Figure 2, which was measured through the same electrical circuit as the detection system, was a little deformed due to the characteristics of the electrical circuits. After stopping the excitation, the detected waveform lasted for more than 50 ms in this case (typical sampling interval of 50 ns for 1 M samples by a digital oscilloscope). The Fourier transform of the detected waveform clearly shows a strong peak at 123.8 kHz due to C_{60} (720 amu).

Because of the strong magnetic field, the radial motion of ions is strongly suppressed. When, two door electrodes further restrict the longitudinal motion of ions, the cluster ions are completely trapped in the ICR cell for a few minutes. We can irradiate laser to the trapped cluster or let the chemical reaction in the cell [Maruyama et al. (1990B), Maruyama et al. (1991)].

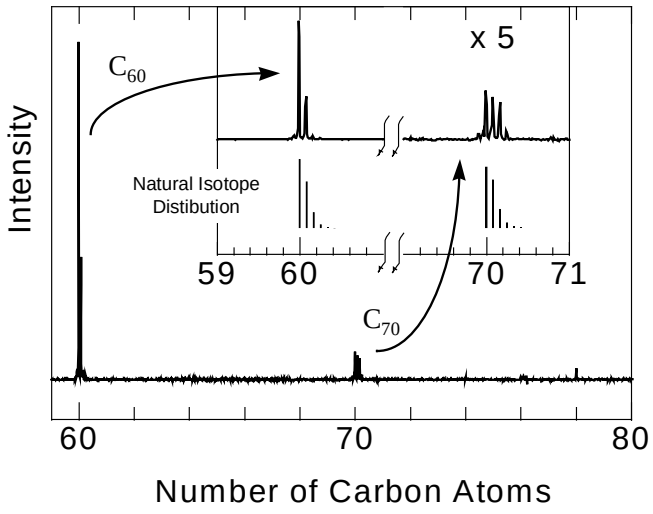

Figure 4 Mass spectrum of extracted fullerene sample.

The schematics of the whole apparatus are shown in Figure 3. The ICR cell was placed in a stainless tube (SUS316)

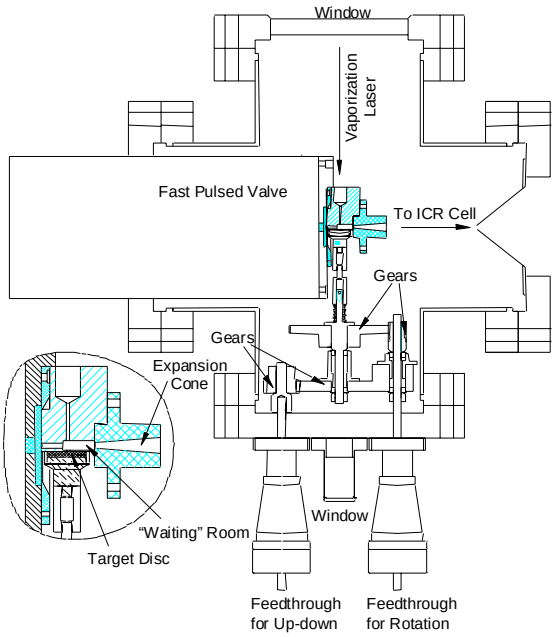

Figure 5 Supersonic laser-vaporization cluster beam source

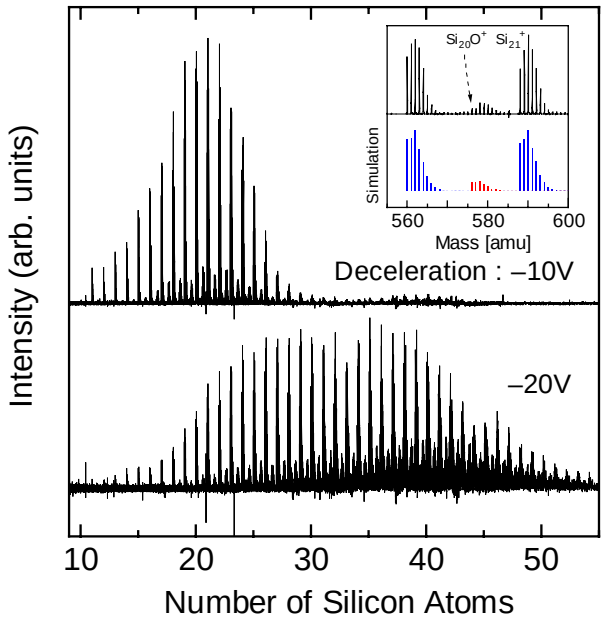

Figure 6 Mass selection by decelerator (silicon clusters)

of id 84 mm which penetrated the homogeneous 6 Tesla superconducting magnet commercially available for NMR. Two turbo-pumps (300 l/s) fore-pumped by a smaller turbo-pump of 50 l/s were placed at the floor in order to avoid the effect of strong magnetic field. The typical background pressure was 3×10^{-10} Torr.

Before setting up the cluster beam source labeled as "Cluster Source" in Figure 3, the direct preparation of cluster ions near the ICR cell was tried by inserting a long tube from the position of cluster source with a sample material on one end near the screen door. By focusing a laser light from the right hand side in Figure 3, the sample material was vaporized. As the first sample, we used silver plate and measured ICR frequency for two natural isotopes Ag^{107} and Ag^{109} for the calibration of the magnetic field. As a result, the effective magnetic field B was measured as 5.804 Tesla compared to the specification of 5.87 Tesla at the initial installation. Considering all spectra in this paper, the effective magnetic field was within ±0.2% which corresponded to about ±2 amu in 1000 amu mass range.

Figure 4 shows an example of the mass spectrum of the fullerene mixture sample made in our arc-discharge fullerene generator (Maruyama et al., 1995). The toluene extract of fullerene was soaked in a graphite disk and dried. The vaporization laser was 2nd harmonics of Nd:YAG (1.5 mJ/pulse focused to about 0.5 mm, 3s irradiation at 10 Hz). We can clearly see the mass peaks of C_{60} and C_{70} as we expected from the HPLC measurements (Maruyama et al., 1995). Here, detailed distributions of C_{60} and C_{70} peaks are shown in the inserted panel in comparison with the theoretical isotope distribution calculated from the natural abundance of C^{13} isotope (1.108 %). The fine distribution due to isotopes was in good agreement, and it was demonstrated that the high mass-resolution of 1 amu was very easily achieved at the 1000 amu range. It should be noted that we have done no adjustments to improve the mass-resolution that was crucial for two-stage acceleration or reflectron TOF mass spectrometer (Maruyama et al., 1997).

CLUSTER BEAM SOURCE AND DIRECT INJECTION

The atomic cluster beam was generated outside of magnetic field by the laser-vaporization cluster beam source shown in Figure 5. The design principle of this cluster source was similar to our previous versions [Maruyama et al. (1990A), Maruyama et al. (1997)]. A pulsed gas valve, the sample motion mechanism and a skimmer are installed in a 6-inch 6-way UHV cross. A solid sample disk was vaporized by the focused beam of laser (2nd Harmonics of Nd:YAG) while timed pulsed gas was injected to the nozzle. In the atmosphere of helium gas, vaporized atoms condensed to clusters, and then, were carried and cooled by the supersonic expansion of helium gas. The cluster beam was skimmed by the skimmer with the opening diameter of 2 mm. The motion mechanism of the sample holder ensured the uniform consumption of the sample material.

The cluster beam was directly injected to the magnetic

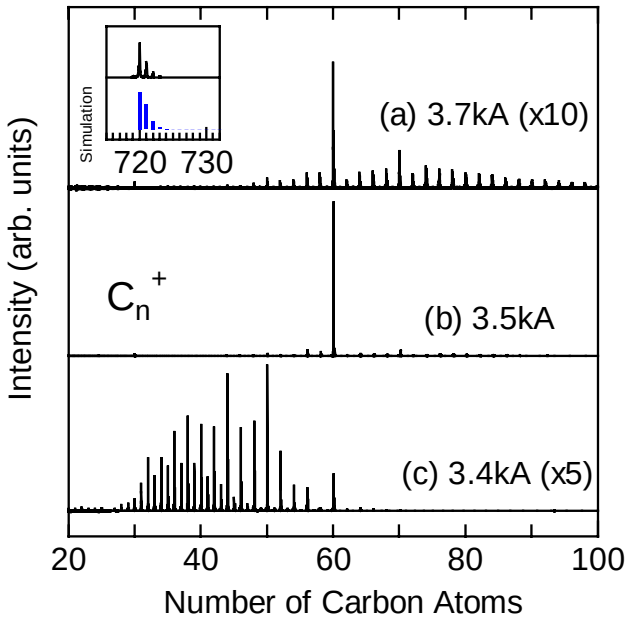

Figure 7 Dependence of Helium gas pressure on the carbon cluster cation mass distribution.

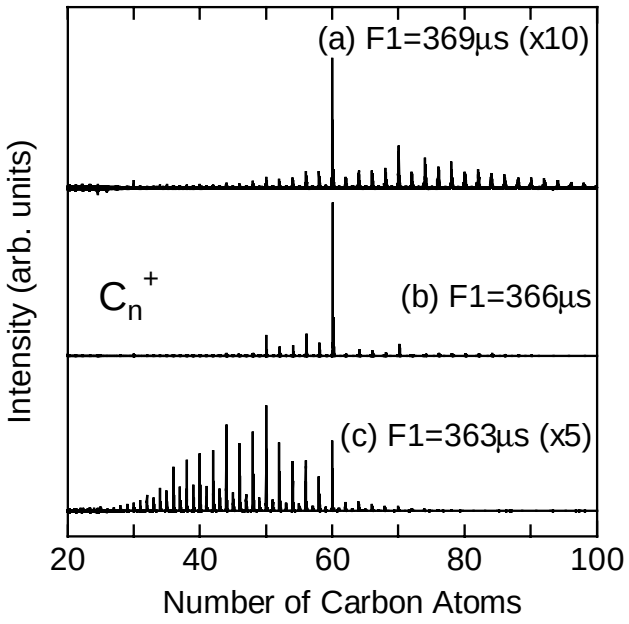

Figure 8 Dependence of vaporization laser irradiation timing relative to gas pulse

field through skimmer and deceleration tube (Maruyama et al., 1990A). Cluster ions carried by the helium gas had almost the supersonic speed of helium. Deceleration tube was kept at 0V until cluster ions came into the middle of the tube. Then, the voltage was suddenly pulsed to a negative potential (for positive ions). Ions felt no field until they climbed up to the voltage of screen door that was typically set to +5 V (for positive ions). Then, cluster ions lost the translational energy at the amount of the pulsed deceleration voltage. The 'front' door was kept typically at +10 V and ramped down to 0V only when injecting the cluster ions. The 'back' door was always kept typically at +10 V. Then, cluster ions which had enough translational energy to climb up the screen door but smaller enough so that reflected by the back door would be trapped in the ICR cell.

An example of the decelerator operation is demonstrated in Figure 6 for silicon clusters, which have no specific mass distribution as carbon [Maruyama et al. (1990A), Maruyama et al. (1990B)]. A silicon wafer cut to a disk was installed in the cluster beam source. With the deceleration voltage of –10 V, those clusters with 15 to 20 eV translational energy should be trapped in the ICR cell as the ideal condition. These corresponded to the mass range of roughly 750 to 1000 amu (or Si_{27} to Si_{36}). In the case of –20V deceleration voltage the simply estimated mass range was Si_{45} to Si_{54}. The measured mass-range in Figure 6 was understandable if we included some loss of translational energy converted to the cyclotron motion. It is clear that the rough selection of mass range was possible by this deceleration tube technique.

In the case of silicon clusters, the isotope distribution is more complicated since the natural abundance of Si isotopes are Si_{28}: 92.23 %, Si_{29}: 4.67 %, Si_{30}: 3.1%. The inserted panel shows the expanded data in comparison with the theoretical isotope distribution. It is also noted that the smaller signal between silicon clusters were oxides Si_nO.

GENERATION OF CARBON CLUSTERS

Examples of carbon mass spectra measured by the direct-injection FT-ICR apparatus are shown in Figure 7. Here, a graphite sample was vaporized by the 2nd harmonics of Nd: YAG laser and the positive carbon clusters were trapped. Figure 7 (a) is very much similar to the well-known positive carbon mass distribution which lead to the discovery of spherical C_{60} structures [Kroto et al. (1985), Rohlfing et al. (1984)]. We can observe completely different aspects of mass spectra for less amount of source helium gas in the nozzle of the laser-vaporization cluster source. The driving current of the pulsed nozzle, which was roughly proportional to the nozzle pressure, was changed in Figure 7. At the condition of Figure 7 (b) almost only C_{60} was observed and the even less pressure lead to the odd number of carbon atoms, which could be regarded as the non-closed structures of positive carbon clusters. These findings of intermediate stage of the fullerene formation must be very important for understandings of the fullerene formation mechanism.

Figure 8 shows the similar results depending on the laser-vaporization timing relative to the helium gas pulse. The

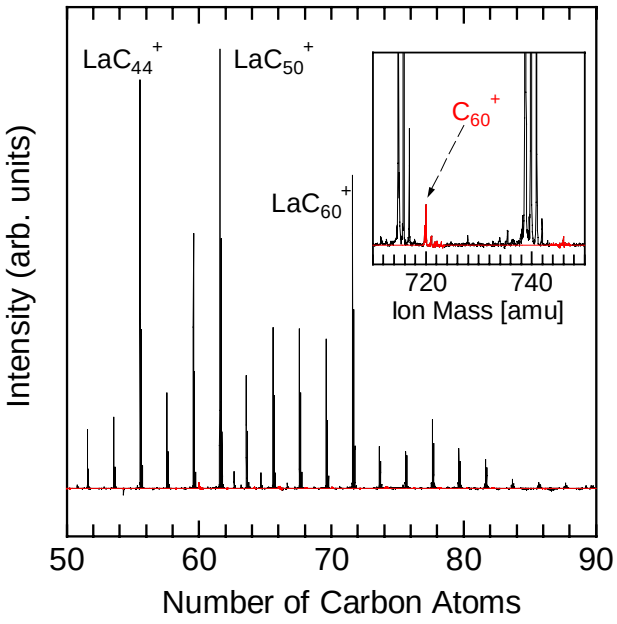

Figure 9 Lanthanum-carbon binary clusters

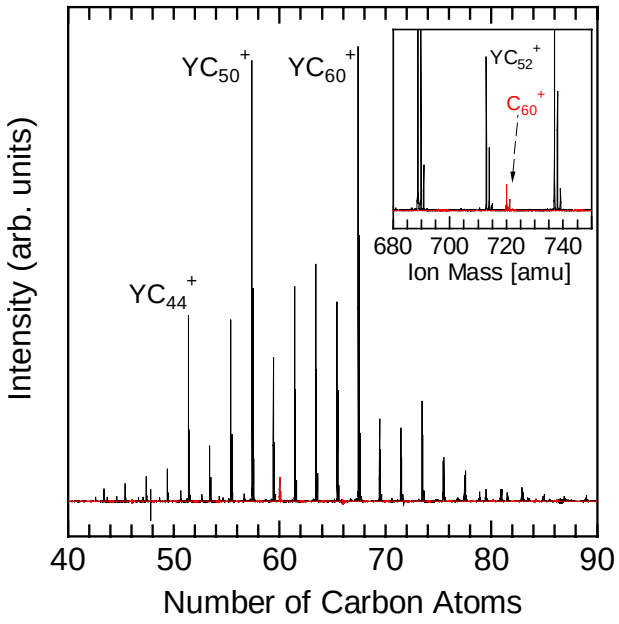

Figure 10 Yttrium-carbon binary cluster.

pressure at the nozzle at the time of vaporization is a complex function of this timing and the nozzle current (Maruyama et al., 1997). However, Figure 7 and Figure 8 show that the decrease of pressure in the nozzle corresponded to the earlier stage of the formation process. It should be noticed that C_{44}, C_{50} and C_{60} were observed to be special magic numbers both in Figure 7 (c) and in Figure 8 (c).

METAL-CARBON BINARY CLUSTERS

Figures 9-11 show mass spectra of metal-carbon binary clusters for La-C (Figure 9), Y-C (Figure 10), and Sc-C (Figure 11). All of these metal atoms are known to be included in fullerene carbon cage [Chai et al. (1991), Kikuchi et al. (1993), Takata et al. (1995)]. Even though the metal-containing fullerene is expected to have very interesting physical and chemical properties, the macroscopic generation of such fullerene is extremely difficult. Typical yield of metal containing fullerene is order of 0.1 % in the arc-discharge fullerene generator. Hence, understandings of the formation mechanism are very much anticipated. The mass-spectroscopic result was very surprising for La-C and Y-C cases. There was only a trace of bare carbon clusters in Figure 9 and Figure 10 (See inserted panels for the extended view of small C_{60} signal). In the case of Sc-C, on the other hand, the bare carbon clusters exhibited almost the same intensity as binary clusters. If we ignore the metal-composite clusters, the distribution of bare carbon clusters was almost the same as typical positive ion clusters. Almost all of metal-carbon composite clusters had only one metal atom and even

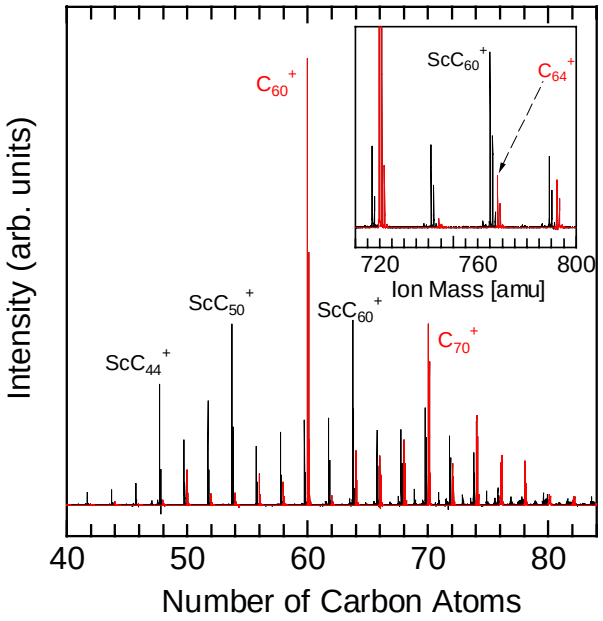

Figure 11 Scandium-carbon binary clusters.

number of carbon atoms: MC_{2n} in the range of $36 \le 2n \le 76$, with special magic numbers of MC_{44}, MC_{50}, MC_{60} (M = La, Y, Sc). These features resembled to the magic number feature observed in Figure 7 (c) and Figure 8 (c) but an addition of a metal atom. The complete lack of odd number carbon clusters might be ascribed to the enhancement of clustering process due to the metal atom. The even number of carbon atoms strongly suggests the hypothesis that all of these

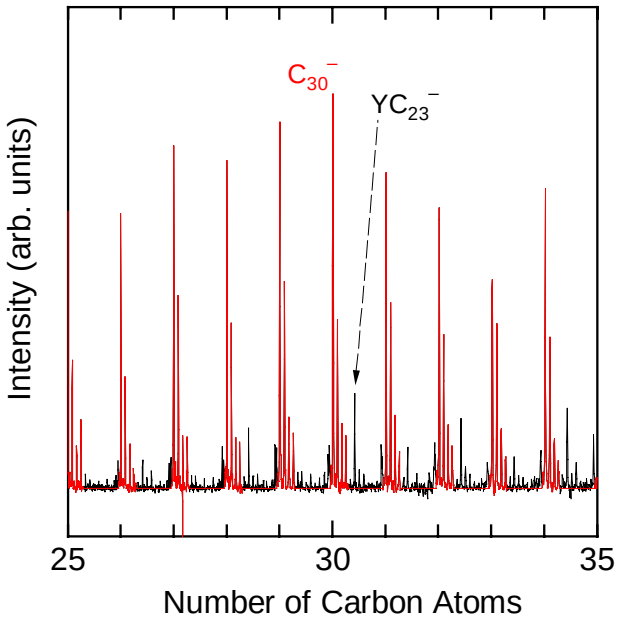

Figure 12 Example of negative cluster mass spectrum for Y-C cluster.

composite clusters have closed caged structure: according to Euler's theorem for a closed polyhedron, the number of atoms must be even when all atoms have three bonds (Maruyama & Yamaguchi, 1998). We expect that these composite clusters should have imperfect fullerene cage with metal atom inside of the cage.

An example of negative cluster mass spectrum for Y-C binary clusters is shown in Figure 12. In order to measure the spectra of negative clusters, simply the polarity of deceleration tube and doors were reversed. Here, the signal of clusters with yttrium is remarkably small in contrast to the positive mass spectrum in Figure 10. In general, the positive and negative mass spectra are considerably different. Since we cannot directly observe the spectra of neutral clusters, it is always frustrating. In order to discuss the formation mechanism, it is most important to explore characteristics of abundant neutral clusters. Positive mass spectra tend to overestimate the clusters with lower ionization potential and on the other hand negative spectra tend to exaggerate low temperature clusters which can easily keep an extra electron. At this stage we believe that the rapid reaction with a metal atom makes the binary clusters too hot to be observed as negative clusters. The systematic studies of both positive and negative clusters in the future is necessary.

CONCLUSIONS

We have successfully implemented the FT-ICR (Fourier Transform Ion Cyclotron) mass spectrometer with direct-injection cluster beam source. The high mass-resolution was demonstrated for positive mass spectra of silicon, carbon, and metal-carbon binary clusters and negative mass spectra of metal-carbon binary clusters. For bare carbon positive clusters, we found the special condition where the odd-numbered clusters were observed in the range of C_{30} to C_{50} and the continuous change to C_{60}-dominant condition and 'normal' even-numbered distribution. The metal-composite clusters showed magic numbers of MC_{44}, MC_{50}, MC_{60} (M = La, Y, Sc). In addition, the possibility of measuring negative cluster ions was also demonstrated.

ACKNOWLEDEMENTS

This work was supported by Grant-in-Aid for Scientific Research (No. 09450085) from the Ministry of Education, Science, Sports and Culture, Japan. One of the author (S. M.) thanks Professor R. E. Smalley at Rice University for discussions and his kind support for the superconducting magnet.

REFERENCES

Chai, Y., Guo, T., Jin, C., Haufler, R. E., Chibante, L. P. F., Fure, J., Wang, L., Alford, J. M. and Smalley, R. E., 1991, "Fullerenes with Metals Inside," *J. Phys. Chem.*, vol. 95, pp. 7564-7568.

Haufler, R. E., Chai, Y., Chibante, L. P. F., Conceicao, J., Jin, C., Wang, L.-S., Maruyama, S. and Smalley, R. E., 1991, "Carbon Arc Generation of C_{60}," *Mat. Res. Soc. Symp. Proc.*, vol. 206, pp. 627-638.

Iijima, S., 1991, "Helical Microtubules of Graphitic Carbon," *Nature*, vol. 354, pp. 56-58.

Kikuchi, K., Nakahara, N., Wakabayashi, T., Honda, M., Matsumiya, H., Moriwaki, T., Suzuki, S., Shiromaru, H., Saito, K., Yamauchi, K., Ikemoto, I. and Achiba, Y., 1992, "Isolation and Identification of Fullerene Family - C_{76}, C_{78}, C_{82}, C_{84}, C_{90} and C_{96}," *Chem. Phys. Lett.*, vol. 188, pp. 177-180.

Kikuchi, K., Suzuki, S., Nakano, Y., Nakahara, N., Wakabayashi, T., Shiromaru, H., Saito, K., Ikemoto, I. and Achiba, Y., 1993, "Isolation and Characterization of the Metallofullerene LaC_{82}," *Chem. Phys. Lett.*, vol. 216, pp. 23-26.

Krätschmer, W., Lamb, L.D., Fostiropoulos, K. and Huffman, D. R., 1990, "Solid C_{60}: a New Form of Carbon," *Nature*, vol. 347, pp. 354-358.

Kroto, H. W., Heath, J. R., O'Brien, S. C., Curl, R. F. and Smalley, R. E., 1985, "C_{60}: Buckminsterfullerene," *Nature*, vol. 318, pp. 162-163.

Marshall, A. G. and Verdun, F. R., 1990, *Fourier Transforms in NMR, Optical, and Mass Spectrometry*, Elsevier, Amsterdam.

Marshall, A. G., Wang, T. C. L. and Ricca, T. L., 1985,

"Tailored Excitation for Fourier Transform Ion Cyclotron Resonance Mass Spectrometry," *J. Am. Chem. Soc.*, vol. 107, p. 7893.

Maruyama, S., Anderson, L. R. and Smalley, R. E., 1990A, "Direct Injection Supersonic Cluster Beam Source for FT-ICR Studies," *Rev. Sci. Instrum.*, vol. 61-12, pp. 3686-3693.

Maruyama, S., Anderson, L. R. and Smalley, R. E., 1990B, "Laser Annealing of Silicon Clusters," *J. Chem. Phys.*, vol. 93-7, pp. 5349-5351.

Maruyama, S., Kinbara, H., Hayashi, H. and Kimura, D., 1997, "Photoionized TOF Mass Spectrometry of Atomic Clusters," *Microscale Thermophysical Engineering*, vol. 1-1, pp. 39-46.

Maruyama, S., Lee, M. Y., Haufler, R. E., Chai, Y. and Smalley, R. E., 1991, "Thermionic Emission from Giant Fullerenes," *Z. Phys. D*, vol. 19, pp. 409-412.

Maruyama, S., Takagi, T., Kaji, Y. and Inoue, M., 1995, "Temperature Field Measurement During the Arc-Discharge Fullerene Generation Process," *Proc. 32nd National Heat Transfer Conf., Japan*, vol. 2, p. 569.

Maruyama, S. and Yamaguchi, Y., 1998, "A Molecular Dynamics Demonstration of Annealing to a Perfect C_{60} Structure," *Chem. Phys. Lett.*, vol. 286-3,4, pp. 343-349.

Rohlfing, E. A., Cox, D. M. and Kaldor, A., 1984, "Production and Characterization of Supersonic Carbon Cluster Beams," *J. Chem. Phys.*, vol. 81, pp. 3322-3330.

Takata, M., Umeda, B., Nishibori, E., Sakata, M., Saito, Y., Ohno, M. and Shinohara, H., 1995, "Confirmation by X-ray Diffraction of the Endohedral Nature of the Metallofullerene $Y@C_{82}$," *Nature*, vol. 377, pp. 46-48.

Thess, A., Lee, R., Nikolaev, P., Dai, H., Petit, P., Robert, J., Xu, C., Lee, Y. H., Kim, S. G., Rinzler, A. G., Colbert, D. T., Scuseria, G. E., Tomanak, D., Fischer, J. E. and Smalley, R. E., 1996, "Crystalline Ropes of Metallic Carbon Nanotubes," *Science*, vol. 273, pp. 483-487.

Wakabayashi, T., Kasuya, D., Shiromaru, H., Suzuki, S., Kikuchi, K. and Achiba, Y., 1997, "Towards the Selective Formation of Specific Isomers of Fullerenes : T- and p-Dependence in the Yield of Various Isomers of Fullerenes C_{60}-C_{84}," *Z. Phys. D*, vol. 40, pp. 414-417.

Yamaguchi, Y. and Maruyama, S., 1998, "A Molecular Dynamics Simulation of the Fullerene Formation Process," *Chem. Phys. Lett.*, vol. 286-3,4, pp. 336-342.

Yamaguchi, Y., Maruyama, S. and Hori, S., 1999, " Molecular Dynamics Simulations of Formation of Metal-Containing Fullerene," *5th ASME/JSME Thermal Engng. Conf.*, San Diego, AJTE99-6508.